Physics Letters B 778 (2018) 447–453

Contents lists available at ScienceDirect

Physics Letters B

www.elsevier.com/locate/physletb

Quark matter and quark stars in strong magnetic fields at finite temperature within the confined-isospin-density-dependent mass model

Peng-Cheng Chu [a,*], Xiao-Hua Li [b,c], Hong-Yang Ma [a], Bin Wang [a], Yu-Min Dong [a], Xiao-Min Zhang [a]

[a] School of Science, Qingdao Technological University, Qingdao 266000, China
[b] School of Nuclear Science and Technology, University of South China, 421001 Hengyang, China
[c] Cooperative Innovation Center for Nuclear Fuel Cycle Technology & Equipment, University of South China, 421001 Hengyang, China

ARTICLE INFO

Article history:
Received 7 December 2017
Received in revised form 8 January 2018
Accepted 22 January 2018
Available online 31 January 2018
Editor: W. Haxton

ABSTRACT

We study the properties of strange quark matter (SQM) and quark stars (QSs) in strong magnetic fields within the extended confined isospin-density-dependent mass (CIDDM) model including the temperature dependence of the equivalent mass for quarks. The quark symmetry energy, quark symmetry free energy, and the equation of state (EOS) of SQM in constant magnetic fields at finite temperature are investigated, and it is found that including the temperature dependence in CIDDM model and considering strong magnetic fields can both significantly influence the properties of the SQM and the maximum mass of quark stars. Using the density-dependent magnetic field and assuming two extreme cases for the magnetic field orientation in QSs (the radial orientation in which the local magnetic fields are along the radial direction and the transverse orientation in which the local magnetic fields are randomly oriented but perpendicular to the radial orientation), we analyze the mass-radius relations for different stages of the protoquark stars (PQSs) along the star evolution. Our results indicate that the maximum mass of magnetized PQSs may depend on not only the strength distribution and the orientation of the magnetic fields inside the PQSs, but also the heating process and the cooling process in the star evolution.

1. Introduction

The investigation of the properties of strong interaction matter is one of the fundamental issues in nuclear physics and astrophysics. In terrestrial laboratories, the experiments of high energy heavy ion collisions (HICs) can provide the unique tool to explore the properties of strong interaction matter. The hot and dense quark matter might be created in HICs from the Nuclotron-based Ion Collider Facility (NICA) at JINR and the Facility for Antiproton and Ion Research (FAIR) at GSI, while the hot quark-gluon plasma (QGP) is expected to be created in HICs at the Large Hadron Collider (LHC) at CERN and the Relativistic Heavy Ion Collider (RHIC) at BNL. In nature, neutron stars (NSs) provide a unique astrophysical testing grounds of our knowledge to explore the properties of strong interaction matter, especially the equation of state (EOS) of neutron-rich matter, at low temperature and high baryon density [1,2].

Theoretically, NSs may be converted to strange quark stars (QSs), which are made of deconfined absolutely stable u, d and s quark matter in β-equilibrium condition, i.e., strange quark matter (SQM). The possible existence of QSs is one of the most intriguing aspects of modern astrophysics and cannot be conclusively ruled out [3–9]. In QSs, there exists large $u-d$ quark asymmetry (isospin asymmetry) in the star matter, which indicates the importance of the isovector properties in SQM, and the numbers of u and d ($\bar{u}$ and $\bar{d}$) quarks can be generally found unequal in high energy HICs at RHIC/LHC, which is also isospin asymmetric. Therefore it is of great interests and critical importance to study the isovector properties of quark star matter (one can describe these properties by studying the quark matter symmetry energy and quark matter symmetry free energy), the isospin-dependence of the QCD phase diagram, and the isospin effects of partonic dynamics in high energy HICs.

* Corresponding author.
E-mail addresses: kyois@126.com (P.-C. Chu), lixiaohuaphysics@126.com (X.-H. Li), hongyang-ma@aliyun.com (H.-Y. Ma), zhangxm@mail.bnu.edu.cn (X.-M. Zhang).

https://doi.org/10.1016/j.physletb.2018.01.064

When massive stars exhaust the fuel supply, the type II supernova explosion is triggered, which will cause the core to be crushed by gravity and may form a newly-born compact star (protoneutron star (PNS) or protoquark star (PQS)) [10–13] or a black hole. At the beginning stage of the birth of a PQS, the lepton number per baryon with the trapped neutrinos is approximately 0.4 and the entropy per baryon is about one [13]. During the following 10–20 seconds, the star matter will be heated by the diffusing neutrinos, and the entropy per baryon will increase to two, while the neutrino fraction is almost zero. Then the PQSs begins cooling down at the third stage and finally forms into the cold QSs [14–16].

In recent decades, the properties of SQM at finite temperature under strong magnetic fields have attracted lots of interests, and the presence of external magnetic field may harden the EOS of SQM when considering that the NSs can be endowed with strong magnetic fields [17], i.e., magnetars. At the surface of the compact star, the magnetic field strength is estimated as $B \sim 10^{14}$ G [18–20], and the magnetic field strength may reach as large as $B \sim 10^{20}$ G in the core of the self-bound QSs [21,22]. Under such strong magnetic fields, the spatial rotational symmetry will break and one should introduce the pressure anisotropy of this system [22–25]. In [26], the authors use a density-dependent magnetic field profile [27,28] and investigate the properties of magnetars by assuming two extreme cases for the orientation inside the quark stars (one is that the local magnetic fields are along the radial direction in QSs, which is denoted as "radial orientation", while the other one is that the magnetic fields are perpendicular to the radial direction but randomly oriented in the plane perpendicular to the radial direction, which is denoted as "transverse orientation") at zero temperature.

In the present work, we extend the confined isospin-density-dependent mass (CIDDM) model to include temperature dependence of the equilibrium mass of quarks to investigate the quark matter symmetry free energy/ symmetry free energy and the equation of state (EOS) for SQM in constant magnetic fields at finite temperature. The properties of PQSs under strong magnetic fields are also studied, and we find that the maximum mass of magnetized PQSs may depend on not only the strength distribution and the orientation of the magnetic fields inside the stars, but also the heating and cooling process in the star evolution.

2. Models and methods

2.1. The confined isospin-density-dependent mass model

The CIDDM model [26,29,30] extends the confined density-dependent mass model (i.e., the CDDM) model [31–39] by including the isospin dependence for the equivalent quark mass. With baryon number density n_B and isospin asymmetry δ, the quark mass can be expressed as

$$\begin{aligned} m_q &= m_{q_0} + m_I + m_{iso} \\ &= m_{q_0} + \frac{D}{{n_B}^z} - \tau_q \delta D_I n_B^\alpha e^{-\beta n_B}, \end{aligned} \tag{1}$$

where m_{q0} is the quark current mass, $m_I = \frac{D}{{n_B}^z}$ represents the flavor-independent quark interactions, while $m_{iso} = -\tau_q \delta D_I n_B^\alpha e^{-\beta n_B}$ is the isospin dependent part. For $m_I = \frac{D}{{n_B}^z}$, z is the equivalent mass scaling parameter and D can be determined by the stability arguments of SQM. For $m_{iso} = -\tau_q \delta D_I n_B^\alpha e^{-\beta n_B}$, the parameters D_I, α and β can determine the isospin-density dependence of the effective interactions in quark matter, τ_q means the isospin quantum number of quarks, and we set $\tau_q = 1$ for $q = u$ (u quarks), $\tau_q = -1$ for $q = d$ (d quarks), and $\tau_q = 0$ for $q = s$ (s quarks). The isospin asymmetry is defined from the works [29,40–43] as

$$\delta = 3\frac{n_d - n_u}{n_d + n_u}. \tag{2}$$

In Eq. (1), the quark confinement condition $\lim_{n_B \to 0} m_q = \infty$ will be guaranteed if the scaling parameter $z > 0$ and $\alpha \geq 0$. In addition, if $\beta > 0$, then $\lim_{n_B \to \infty} m_{iso} = 0$, which satisfies the asymptotic freedom $\lim_{n_B \to \infty} m_q = m_{q0}$. The readers are referred to Ref. [29] for more details about the CIDDM model.

Using the similar way as in Ref. [44] and Ref. [45], we introduce the temperature dependence of equivalent mass for quarks in the CIDDM model by considering the linear confinement and string tension $\sigma(T)$, and the equivalent quark mass is modified as

$$m_q = m_{q_0} + \left(\frac{D}{{n_B}^z} - \tau_q \delta D_I n_B^\alpha e^{-\beta n_B} \right) \sigma(T), \tag{3}$$

with

$$\sigma(T) = 1 - \frac{8T}{\lambda T_c} \exp\left(-\lambda \frac{T_c}{T} \right), \tag{4}$$

where $q = u, d, s$, $\sigma(T)$ is the temperature dependent string tension [46], $T_c = 170$ MeV is the critical temperature calculated from LQCD [47], and $\lambda = 1.605812$ is determined as the solution of the equation $1 - \frac{8T}{\lambda T_c} \exp(-\lambda \frac{T_c}{T}) = 0$ when $T = T_c$. One can find that m_q decreases as temperature increases, and the equivalent mass will reach the quark current mass m_{q0} when temperature hits the critical value T_c, which shows the chiral symmetry restoration feature.

2.2. Properties of SQM

The weak beta-equilibrium condition for SQM (we assume it is composed of u, d, and s quarks and e, μ, ν_e and ν_μ leptons with electric charge neutrality in beta-equilibrium) can be expressed as

$$\mu_d = \mu_s = \mu_u + \mu_e - \mu_{\nu_e}, \tag{5}$$

$$\mu_\mu = \mu_e \quad \text{and} \quad \mu_{\nu_\mu} = \mu_{\nu_e}. \tag{6}$$

And the electric charge neutrality condition can be written as

$$\frac{2}{3} n_u = \frac{1}{3} n_d + \frac{1}{3} n_s + n_e + n_\mu. \tag{7}$$

In an external constant magnetic field with strength B, the energy spectrum for quarks and leptons with electric charge q_i can be expressed as [48]

$$E_{p,i} = \sqrt{p_z^2 + 2\nu |q_i| B + m_i^2}, \tag{8}$$

where m_i is the quark mass, p_z is the momentum in the z direction (the magnetic field is assumed to be along the z axis), $\nu = n + \frac{1}{2} - \frac{q_i}{|q_i|}\frac{s}{2}$ is the Landau levels with $n = 0, 1, 2, 3, \ldots$ being the principal quantum number, and $s = +1$ for spin-up while $s = -1$ for spin-down. In this paper, we do not consider the contributions from the anomalous magnetic moments because the anomalous magnetic moments are not well understood in for quark matter in the deconfined condition and are not important for leptons [25,27,28,49–52].

The total thermodynamic potential density for SQM at finite temperature under strong magnetic fields can be written as

$$\Omega = \sum_i \Omega_i, \tag{9}$$

where i in the sum is for all flavors of quarks (u, d, and s) and leptons (e, μ, ν_e, and ν_μ). Then the contribution of the particle with flavor i to the thermodynamic potential density is

$$\Omega_i = -\sum_\nu \frac{g_i(|q_i|B)T}{2\pi^2}\alpha_\nu \int_0^\infty \{\ln[1+e^{-(E_{p,i}-\mu_i^*)/T}] + \ln[1+e^{-(E_{p,i}+\mu_i^*)/T}]\}\mathrm{d}p_z, \tag{10}$$

where $\alpha_\nu = 2-\delta_{\nu,0}$, μ_i^* is the effective chemical potential (the form of the effective chemical potential for leptons is identical to the form of their chemical potential), and g_i is the value of the degeneracy factor for quarks ($g_i = 3$) and leptons ($g_i = 1$).

For the particle with flavor i, the number density can be obtained as

$$n_i = \sum_\nu \frac{g_i(|q_i|B)}{2\pi^2}\alpha_\nu \int_0^\infty [\frac{1}{1+e^{(E_{p,i}-\mu_i^*)/T}} - \frac{1}{1+e^{(E_{p,i}+\mu_i^*)/T}}]\mathrm{d}p_z. \tag{11}$$

And for the massless neutrinos, the thermodynamic potential density and number density are

$$\Omega_i = -\frac{g_i T}{2\pi^2}\int_0^\infty \{\ln[1+e^{-(p-\mu_i^*)/T}] + \ln[1+e^{-(p+\mu_i^*)/T}]\}p^2\mathrm{d}p, \tag{12}$$

and

$$n_i = \frac{g_i}{2\pi^2}\int_0^\infty [\frac{1}{1+e^{(p-\mu_i^*)/T}} - \frac{1}{1+e^{(p+\mu_i^*)/T}}]p^2\mathrm{d}p. \tag{13}$$

The total free-energy density $\mathcal{F}$ is

$$\mathcal{F} = \sum_i \mathcal{F}_i = \sum_i(\Omega_i + \mu_i^* n_i) + \frac{B^2}{2}, \tag{14}$$

where the term $B^2/2$ comes from the magnetic field contribution.

For SQM under strong magnetic field, the $\mathcal{O}(3)$ rotational symmetry is broken and the pressure for SQM becomes anisotropic. The anisotropic pressure may be split into the longitudinal pressure $P_\parallel$ which is parallel to the magnetic field and the transverse pressure $P_\perp$ which is perpendicular to the magnetic field, and for a magnetized fermion system the expressions of $P_\parallel$ and $P_\perp$ can be written as [22]

$$P_\parallel = -\sum_{i=u,d,s,l}\Omega_i + \sum_{i,j=u,d,s}\frac{\partial\Omega_j}{\partial m_j}\frac{\partial m_j}{\partial n_i}n_i - \frac{B^2}{2}, \tag{15}$$

$$P_\perp = -\sum_{i=u,d,s,l}\Omega_i + \sum_{i,j=u,d,s}\frac{\partial\Omega_j}{\partial m_j}\frac{\partial m_j}{\partial n_i}n_i + \frac{B^2}{2} - MB, \tag{16}$$

where the system magnetization M is given by

$$M = -\partial\Omega/\partial B = \sum_{i=u,d,s,l} M_i. \tag{17}$$

One can find that the magnetic energy density term $B^2/2$ contributes oppositely to the longitudinal and transverse pressures under a constant magnetic field, which will lead to a tremendous difference between the longitudinal and transverse pressure ($P_\parallel < P_\perp$) when the magnetic field becomes strong.

Using $\mu_i = \mathrm{d}\mathcal{F}/\mathrm{d}n_i$, the effective chemical potential for u, d, and s quarks at finite temperature under magnetic field can be expressed as

$$\mu_u^* = \mu_u - \Big\{\frac{1}{3}\sum_{j=u,d,s}\frac{\partial\Omega_j}{\partial m_j} \times\Big[-\frac{zD}{n_B^{(1+z)}} - \tau_j D_I\delta(\alpha n_B^{\alpha-1} - \beta n_B^\alpha)e^{-\beta n_B}\Big] + D_I n_B^\alpha e^{-\beta n_B}\Big(\frac{\partial\Omega_u}{\partial m_u} - \frac{\partial\Omega_d}{\partial m_d}\Big) \times\frac{6n_d}{(n_u+n_d)^2}\Big\}\times\Big[1-\frac{8T}{\lambda T_c}exp(-\lambda\frac{T_c}{T})\Big], \tag{18}$$

$$\mu_d^* = \mu_d - \Big\{\frac{1}{3}\sum_{j=u,d,s}\frac{\partial\Omega_j}{\partial m_j} \times\Big[-\frac{zD}{n_B^{(1+z)}} - \tau_j D_I\delta(\alpha n_B^{\alpha-1} - \beta n_B^\alpha)e^{-\beta n_B}\Big] + D_I n_B^\alpha e^{-\beta n_B}\Big(\frac{\partial\Omega_d}{\partial m_d} - \frac{\partial\Omega_u}{\partial m_u}\Big) \times\frac{6n_u}{(n_u+n_d)^2}\Big\}\times\Big[1-\frac{8T}{\lambda T_c}exp(-\lambda\frac{T_c}{T})\Big], \tag{19}$$

and

$$\mu_s^* = \mu_s - \frac{1}{3}\sum_{j=u,d,s}\frac{\partial\Omega_j}{\partial m_j} \times\Big[-\frac{zD}{n_B^{(1+z)}} - \tau_j D_I\delta(\alpha n_B^{\alpha-1} - \beta n_B^\alpha)e^{-\beta n_B}\Big] \times\Big[1-\frac{8T}{\lambda T_c}exp(-\lambda\frac{T_c}{T})\Big]. \tag{20}$$

The energy density is $\mathcal{E} = \sum_i \mathcal{E}_i$ with

$$\mathcal{E}_i = -\sum_\nu \frac{g_i(|q_i|B)}{2\pi^2}\alpha_\nu\int_0^\infty\Big[\frac{E_{p,i}}{1+e^{(E_{p,i}-\mu_i^*)/T}} + \frac{E_{p,i}}{1+e^{(E_{p,i}+\mu_i^*)/T}}\Big]\mathrm{d}p_z - T\frac{\partial\Omega_i}{\partial m_i}\frac{\partial m_i}{\partial T} + \frac{B^2}{2}. \tag{21}$$

And the entropy density can be calculated as

$$S = \sum_i S_i = \sum_i(-\frac{\partial\Omega_i}{\partial T} - \frac{\partial\Omega_i}{\partial m_i}\frac{\partial m_i}{\partial T}), \tag{22}$$

where

$$\frac{\partial\Omega_i}{\partial m_i} = \sum_\nu \alpha_\nu\frac{g_i|q_i|B}{2\pi^2}\int_0^\infty\Big[\frac{1}{1+e^{(E_{p,i}-\mu_i^*)/T}} + \frac{1}{1+e^{(E_{p,i}+\mu_i^*)/T}}\Big]\frac{1}{E_{p,i}}\mathrm{d}p_z, \tag{23}$$

and

$$\frac{\partial\Omega_i}{\partial T} = -\sum_\nu \alpha_\nu \frac{g_i|q_i|B}{2\pi^2}\int_0^\infty \Big\{\ln\Big[1+e^{-(E_{p,i}-\mu_i^*)/T}\Big] + \frac{(E_{p,i}-\mu_i^*)/T}{1+e^{(E_{p,i}-\mu_i^*)/T}} + \ln\Big[1+e^{-(E_{p,i}+\mu_i^*)/T}\Big] + \frac{(E_{p,i}+\mu_i^*)/T}{1+e^{(E_{p,i}+\mu_i^*)/T}}\Big\} dp_z. \quad (24)$$

From the equation $\mathcal{F} = \mathcal{E} - TS$, one can find that the value of energy density is identical to the value of free energy density when $T = 0$.

2.3. Density-dependent magnetic fields in quark stars

As it is accepted, the magnetic field strength in the inner core of compact stars should be much larger than that at the surface, and people usually propose a density-dependent magnetic field distribution to describe the spatial distribution of the magnetic field strength [17,26,27]. In this work, we use the following density-dependent magnetic field profile inside the PQSs as in Ref. [17,27,28,53,54]

$$B = B_{surf} + B_0[1 - \exp(-\beta_0(n_B/n_0)^\gamma)], \quad (25)$$

where B_{surf} is the magnetic field strength at the surface of compact stars and its value is fixed conventionally at $B_{surf} = 10^{15}$ G in the present work, B_0 is a parameter with dimension of B, $n_0 = 0.16$ fm^{-3} is the normal nuclear matter density, β_0 and γ are two dimensionless parameters that control the density dependence of the magnetic field strength from the center to the surface. In Ref. [26], the authors assume two extremely special cases for the orientation distribution inside QSs: one is that the local magnetic fields are along the radial direction in QSs, which is denoted as "radial orientation", and the other is that the magnetic fields are perpendicular to the radial direction but randomly oriented in the plane perpendicular to the radial direction, which is denoted as "transverse orientation". By using the EOS for SQM at finite temperature and considering the density-dependent magnetic fields, people can obtain the properties of the PQSs under strong magnetic fields by solving Tolman–Oppenheimer–Volkoff (TOV) equations [55].

At the very beginning stage of the birth for the PQSs, the number of leptons per baryon with trapped neutrinos is about $0.4(Y_l = Y_e + Y_\mu + Y_{\nu_l} = Y_e + Y_\mu + Y_{\nu_e} + Y_{\nu_\mu} = 0.4)$ and the entropy per baryon is about one, which is considered as the first snapshot of PQS evolution [15,56]. During the following 10–20 seconds, neutrinos can escape from the star and the diffusing neutrinos will heat the star matter [10], which increase the corresponding entropy per baryon to 2. In this stage, the neutrino fraction is almost zero, and this is the second snapshot of PQS evolution. Following the heating stage, the star begins cooling down, then finally a cold quark star forms [15,56]. In this work, we describe the star evolution for PQSs by using three snapshots:

(I) $S/n_B = 1$, $Y_l = 0.4$, (26)

(II) $S/n_B = 2$, $Y_{\nu_l} = 0$, (27)

(III) $S/n_B = 0$, $Y_{\nu_l} = 0$. (28)

3. Results and discussions

Following the Ref. [29], the set of parameters we used is: $m_{u0} = m_{d0} = 5.5$ MeV, $m_{s0} = 80$ MeV, $m_e = 0.511$ MeV, and $m_\mu = 105.7$ MeV. We also choose a typical set of parameters from [29]: DI-85 with $D_I = 85$, $D = 22.922$ MeV fm^{-3z}, $\alpha = 0.7$, $\beta = 0.1$ fm^3, and $z = 1.8$. This parameter set can be used to describe the recently discovered large-mass pulsar PSR J0348+ 0432 with the mass of $2.01 \pm 0.04\ M_\odot$ [57] as a QS at zero temperature within CIDDM model, and by using DI-85 the two-flavor $u-d$ quark matter symmetry energy is larger than about twice that of a free quark gas or normal quark matter within the conventional NJL model. Following Farhi and Jaffe [7], the absolute stability of SQM requires that the minimum energy per baryon of SQM should be less than the minimum energy per baryon of observed stable nuclei, i.e., $M(^{56}Fe)c^2/56 = 930$ MeV, and the minimum energy per baryon of the β-equilibrium two-flavor $u-d$ quark matter should be larger than 930 MeV to be consistent with standard nuclear physics. In [58] and [59], the authors calculate the absolute window for SQM within different phenomenonlogical models, and in this work the EoS for SQM can also satisfy the absolutely stable condition by using DI-85.

3.1. The quark matter symmetry energy and symmetry free energy

The energy per baryon of quark matter can be expanded in isospin asymmetry δ under zero magnetic fields as

$$E(n_B, \delta, n_s) = E_0(n_B, n_s) + E_{\rm sym}(n_B, n_s)\delta^2 + \mathcal{O}(\delta^4), \quad (29)$$

where $E_0(n_B, n_s) = E(n_B, \delta = 0, n_s)$ is the binding energy per baryon number with an equal fraction of u and d quarks. This definition is similar to the case of nuclear matter [60] and the quark matter symmetry energy is expressed as

$$E_{\rm sym}(n_B, n_s) = \frac{1}{2!}\frac{\partial^2 E(n_B, \delta, n_s)}{\partial\delta^2}\bigg|_{\delta=0}. \quad (30)$$

The quark matter symmetry free energy F_{sym} can also be expressed as

$$F_{\rm sym} = \frac{1}{2!}\frac{\partial^2 F}{\partial\delta^2}\bigg|_{\delta=0}, \quad (31)$$

where F is the free energy per baryon for quark matter. One can find that there should be a temperature dependent difference between symmetry free energy and symmetry energy once finite temperature condition is considered, while the symmetry free energy and symmetry energy will have the same value at zero temperature when the entropy density is zero. In Eq. (29), the absence of odd-order terms in δ is due to the exchange symmetry between u and d quarks in quark matter when one neglects the Coulomb interaction among quarks. For quark matter under strong magnetic fields, the exchange symmetry will be violated because the electric charge for u and d quarks are different (this will cause u and d quarks to act differently in quark matter under strong magnetic fields), and then there might exist a linear term $E_{\rm vio}\ \delta$ in Eq. (29). In this work, we still use the conventional definitions of the symmetry energy and symmetry free energy (which is the coefficient of the δ^2 term in Eq. (29)) for simplicity in order to show a direct comparison for $E_{\rm sym}$ and $F_{\rm sym}$ between zero magnetic field case and strong magnetic field case.

In Fig. 1, we calculate the two-flavor $u-d$ quark matter symmetry free energy and symmetry energy as functions of temperature in constant magnetic fields with strengthes of $B = 0$, $B = 2\times10^{18}$ G and $B = 3\times10^{18}$ G within CIDDM model with DI-85, when the baryon density is 1.5 fm^{-3}. In DI-85, we set $\alpha = 0.7$, $\beta = 0.1$ fm^3 to follow the density dependence of the quark matter symmetry energy of a free Fermi gas or the conventional NJL model [29]. In [29], the authors can describe a two solar mass

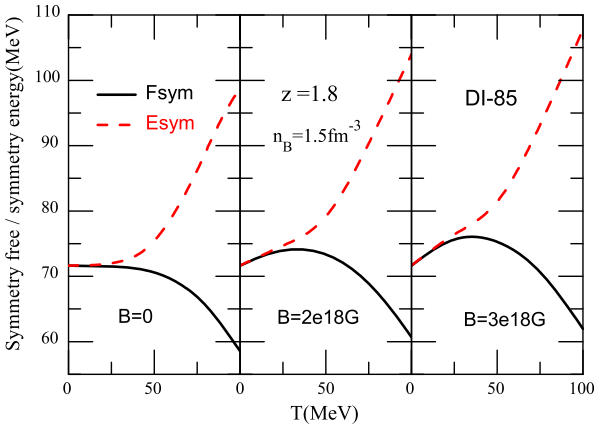

Fig. 1. (Color online) Two-flavor $u-d$ quark matter symmetry free energy (solid lines) and symmetry energy (dashed lines) as functions of temperature in constant magnetic fields with strengthes of $B=0$, $B=2\times10^{18}$ G and $B=3\times10^{18}$ G within CIDDM model with DI-85, when the baryon density is set as 1.5 fm^{-3}.

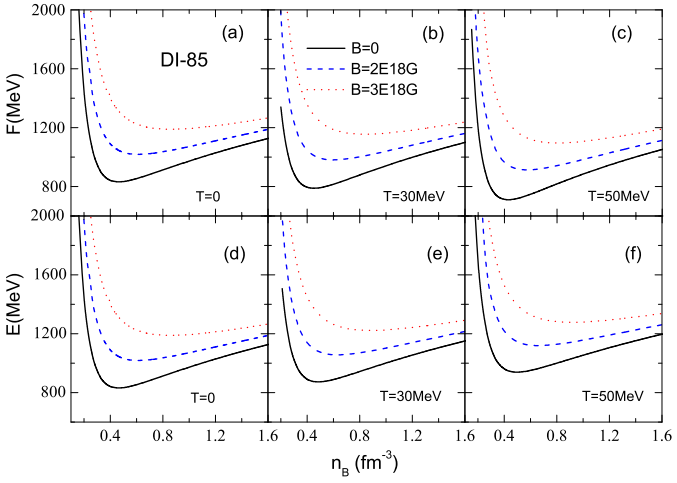

Fig. 2. (Color online) Energy per baryon and free energy per baryon as functions of the baryon density for SQM in constant magnetic fields with strengthes of $B=0$, $B=2\times10^{18}$ G and $B=3\times10^{18}$ G within the CIDDM model with DI-85 at different temperature.

quark star by using DI-85 within CIDDM model with zero temperature and zero magnetic field at $n_B=1.5$ fm^{-3}, and the quark matter symmetry energy is larger than about twice that of a free quark gas or normal quark matter within the conventional NJL model. In order to show a direct comparison, we fix the baryon density for quark matter at 1.5 fm^{-3}.

One can find from the $B=0$ case in Fig. 1 that the value of two-flavor $u-d$ quark matter symmetry free energy decreases with temperature, while the value of symmetry energy increases. As demonstrated in $B=2\times10^{18}$ G and $B=3\times10^{18}$ G cases, the values of the symmetry energy and the symmetry free energy are both enhanced by the magnetic field at a certain temperature, which indicates an obvious magnetic catalysis phenomenon for the symmetry energy and symmetry free energy within the CIDDM model with DI-85.

3.2. EOS of SQM in a constant magnetic field

As shown in Fig. 2 and Fig. 3, we calculate the energy per baryon, the free energy per baryon, and the corresponding longitudinal and transverse pressures as functions of the baryon density for SQM within CIDDM model with DI-85 in constant magnetic

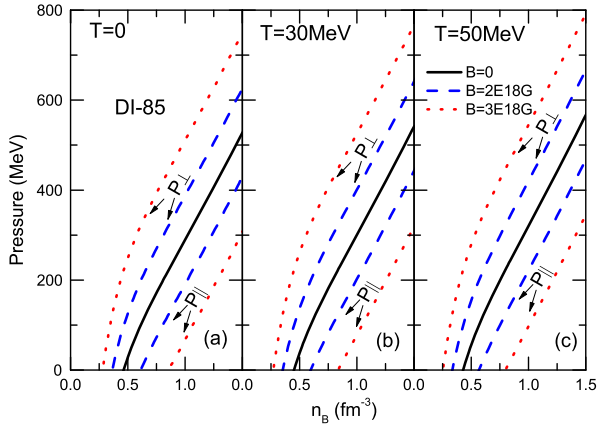

Fig. 3. (Color online) The corresponding longitudinal and transverse pressure as functions of the baryon density for SQM in constant magnetic fields with strengthes of $B=0$, $B=2\times10^{18}$ G, $B=3\times10^{18}$ G within the CIDDM model with DI-85 at different temperature.

fields ($B=0$, $B=2\times10^{18}$ G and $B=3\times10^{18}$ G) at different temperatures. We can obtain the following information from this two figures: (1) The density at the minimum values of the energy per baryon and the free energy per baryon are both equal to the zero-point density of the pressure for $T=0$ and $B=0$ case, which is consistent with the thermodynamic self-consistency and the Hugenholtz–Van Hove (HVH) theorem, while the zero-pressure point is exactly located at the minimum value on every free energy per baryon line in $T=30$ MeV, $B=0$ and $T=50$ MeV, $B=0$ cases. Due to the relation $\mathcal{F}_i=\mathcal{E}_i-TS_i$, the minimum value of the energy per baryon for SQM and the zero-pressure point will not coincide at finite temperature. (2) One can find that the minimum of free energy per baryon decreases with the increment of the temperature, while the minimum of energy per baryon increases. (3) For the constant magnetic field cases $B=2\times10^{18}$ G and $B=3\times10^{18}$ G, the pressure of the system becomes anisotropic, and one can find that the density at the minimum of free energy per baryon is exactly equal to the zero longitudinal pressure point, which is also consistent with the HVH theorem. (4) In addition, the minimum of free energy per baryon and the minimum energy per baryon both increase with the magnetic fields at a fixed temperature, which is consistent with the magnetic catalysis for quark matter symmetry free energy and symmetry energy. And the transverse pressure $P_\perp$ increases with magnetic fields at a fixed baryon density, while the longitudinal pressure $P_{||}$ decreases with magnetic fields, which leads to a clear splitting between $P_\perp$ and $P_{||}$ in constant magnetic fields. Furthermore, the values of $P_\perp$ and $P_{||}$ both increase with temperature when magnetic field is fixed.

In order to clarify the difference for the entropy per baryon in SQM between the magnetized case and the non-polarized state case ($B=0$), we set $\delta S/n_B=[S(T,B)-S(T,B=0)]/n_B$ and calculate $\delta S/n_B$ at different temperature and magnetic field cases in SQM within CIDDM. For $T=30$ MeV, we can obtain $\delta S/n_B=0.024>0$ at $3n_0$ when considering $B=2\times10^{18}$ G and $B=0$ cases, while we can obtain $\delta S/n_B=0.041>0$ at $3n_0$ when considering $B=2\times10^{18}$ G and $B=0$ cases for $T=50$ MeV. This result indicates that the entropy of strongly magnetized quark matter can be larger than the entropy of the non-polarized matter in CIDDM, which is consistent with the result in nuclear matter from the work [23].

3.3. Quark stars at finite temperature under strong magnetic fields

Before we calculate the three snapshots in time evolution of PQSs within the CIDDM model, we first study the properties of

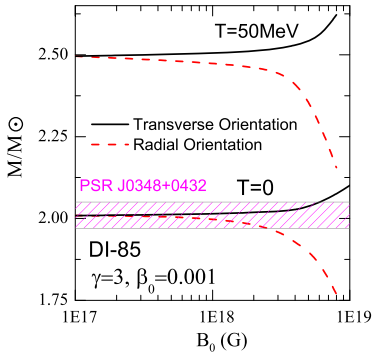

Fig. 4. (Color online) Maximum mass of static QSs using the transverse and radial orientations of the magnetic fields as a function of B_0 within the CIDDM model with DI-85 at different temperature.

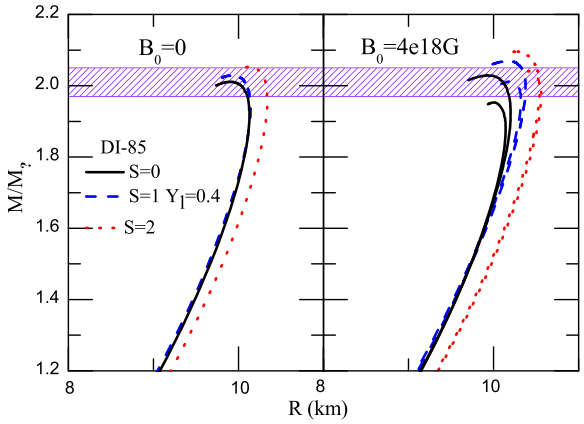

Fig. 5. (Color online) Mass-radius relations of PQSs at three snapshots along the evolution of PQS within CIDDM model with DI-85. The shaded band is the pulsar mass of $2.01 \pm 0.04 M_\odot$ from PSR J0438+0432 [57].

quark stars in finite temperature and strong magnetic field cases. Shown in Fig. 4 is the maximum mass of static QSs using the transverse and radial orientations of the magnetic fields as a function of B_0 within the CIDDM model. We use the fast B-profile (this profile can give a stronger density dependence for magnetic field strength by setting $\gamma = 3$ and $\beta_0 = 0.001$, which indicates obvious effects of density-dependent magnetic fields) from the Ref. [26]. One can find in Fig. 4 that the maximum mass of static QSs increases with B_0 for the transverse orientation at a fixed temperature, while the maximum mass of static QSs decreases with B_0 for the radial orientation, which implies a mass asymmetry for static QSs in strong magnetic fields. In order to observe the effects of the magnetic field orientation on the maximum mass of QSs, the normalized mass asymmetry δ_m is defined as

$$\delta_m = \frac{M_\perp - M_{||}}{(M_\perp + M_{||})/2}, \tag{32}$$

where $M_\perp$ ($M_{||}$) represents the maximum mass of QSs by considering the transverse (radial) orientation. In $T = 0$ case in Fig. 4, δ_m increases with B_0, and the largest mass asymmetry is $\delta_m = 22\%$ at $B_0 = 1 \times 10^{19}$ G with $M_\perp$ ($M_{||}$) reaching about 2.10 $M_\odot$ (1.69 $M_\odot$). As temperature increases, the maximum mass of static QSs for transverse (radial) orientation increases, and the largest mass asymmetry is $\delta_m = 28\%$ at $B_0 = 1 \times 10^{19}$ G with $M_\perp$ ($M_{||}$) reaching about 2.685 $M_\odot$ (2.023 $M_\odot$). Our results indicate that the maximum mass of the magnetized QSs may depend on the strength distribution, the orientation of the magnetic fields inside the magnetars, and the temperature of the QSs.

Shown in Fig. 5 is the mass-radius relations of PQSs at three snapshots along the evolution of PQS within CIDDM model with DI-85 by using transverse and radial orientations of the magnetic fields. For the first stage of the evolution of PQSs with $B_0 = 0$ in the left panel, where the lepton fraction is 0.4 and the entropy per baryon is 1, the maximum mass of the PQSs is 2.03 $M_\odot$. At the second stage of the evolution, the neutrinos diffuse and the entropy per baryon reaches 2, and then the maximum mass of PQSs increases to 2.05 $M_\odot$, which is the largest maximum mass case from all the three stages along the evolution. At the third stage, the star begins cooling down to zero temperature case ($S = 0$) and the maximum mass of PQS is 2.01 $M_\odot$. When the density dependent magnetic field is considered, one can obtain the maximum mass of the magnetars from the right panel, where we use the fast B-profile and set $B_0 = 4 \times 10^{18}$ G within CIDDM model with DI-85. It is seen that the maximum mass of PQS with the transverse (radial) orientation can reach about 2.07 $M_\odot$ (2.01 $M_\odot$) with $B_0 = 4 \times 10^{18}$ G at the first stage, and the mass asymmetry for PQS in strong magnetic field is $\delta_m = 3\%$. For the second stage, $M_\perp$ ($M_{||}$) increases to 2.10 $M_\odot$ (2.04 $M_\odot$) with $\delta_m = 2.9\%$, while $M_\perp = 2.03$ $M_\odot$, $M_{||} = 1.96$ $M_\odot$, and $\delta_m = 3.5\%$ for the third stage with $B_0 = 4 \times 10^{18}$ G. Therefore, our results indicate that the maximum mass of magnetized PQSs may depend on the strength distribution and the orientation of the magnetic fields inside the PQSs, and the heating process in the evolution can also increase the maximum mass of PQSs.

4. Conclusion and discussion

In this work, we have studied the properties of SQM and QSs in strong magnetic fields within the extended CIDDM model including the temperature dependence of the equivalent mass for quarks. The quark matter symmetry free energy and quark matter symmetry energy for asymmetric $u - d$ quark matter at finite temperature under constant magnetic fields have been calculated, and we have found that both the values of the quark matter symmetry free energy and the quark matter symmetry energy increase with the constant magnetic field, which indicates an obvious magnetic catalysis phenomenon. The EOS of SQM has been calculated with self-consistency, and the pressure of the system is anisotropic along or perpendicular to the magnetic field.

We have furthered studied the maximum mass of magnetars within the CIDDM model at finite temperatures by using a density-dependent magnetic field inside the star. We have found that the maximum mass of static QSs increases with B_0 for the transverse orientation case (the local magnetic fields are perpendicular to the radial direction but oriented randomly in the plane perpendicular to the radial direction) at a fixed temperature, while the maximum of static QSs decreases with B_0 for the radial orientation (the local magnetic fields are along the radial direction inside the star), which shows an obvious mass asymmetry for QSs in strong magnetic fields. Under a fixed magnetic field, the maximum mass of static QSs for transverse (radial) orientation increases with the increment of the temperature.

We have also studied the maximum mass of PQSs under density-dependent magnetic fields by considering three different snapshots along the evolution line of stars. We have demonstrated that the maximum mass of PQS increases in the heating stages at a certain B_0, and then the mass asymmetry occurs and increases with B_0 at a fixed stage.

Therefore, our results have shown that considering strong magnetic fields and finite temperature in quark matter within CIDDM model can significantly influence the values of quark matter symmetry free energy, quark matter symmetry energy, properties of the equation of state in SQM, and the maximum mass of static

QSs. The maximum mass of magnetized PQSs may depend on not only the strength distribution and the orientation of the magnetic fields inside the PQSs, but also the heating process and the cooling process in the star evolution.

Acknowledgements

This work is supported by the NSFC under Grant Nos. 11505100, 11547035, 61303256, 61772295, 61605225, 11604174, 11605100 and 61572270, Natural Science Foundation of Shanghai (No. 16ZR1448400), and the Natural Science Foundation of Shandong, China (ZR2015AQ007).

References

[1] J.M. Lattimer, M. Prakash, Science 304 (2004) 536.
[2] A.W. Steiner, M. Prakash, J.M. Lattimer, P.J. Ellis, Phys. Rep. 410 (2005) 325.
[3] D. Ivanenko, D.F. Kurdgelaidze, Lett. Nuovo Cimento 2 (1969) 13.
[4] N. Itoh, Prog. Theor. Phys. 44 (1970) 291.
[5] A.R. Bodmer, Phys. Rev. D 4 (1971) 1601.
[6] E. Witten, Phys. Rev. D 30 (1984) 272.
[7] E. Farhi, R.L. Jaffe, Phys. Rev. D 30 (1984) 2379.
[8] C. Alcock, E. Farhi, A. Olinto, Astrophys. J. 310 (1986) 261.
[9] F. Weber, Prog. Part. Nucl. Phys. 54 (2005) 193.
[10] M. Prakash, I. Bombaci, M. Prakash, P.J. Ellis, J.M. Lattimer, R. Knorren, Phys. Rep. 280 (1) (1997).
[11] V.K. Gupta, Asha Gupta, S. Singh, J.D. Anand, Int. J. Mod. Phys. D 12 (2003) 583–595.
[12] V. Dexheimer, J.R. Torres, D.P. Menezes, Eur. Phys. J. C 73 (2013) 2569.
[13] D.P. Menezes, A. Deppman, E. Megias, L.B. Castro, arXiv:1410.2264v2.
[14] A.W. Steiner, M. Prakash, J.M. Lattimer, Phys. Lett. B 486 (2000) 239.
[15] S. Reddy, M. Praskash, J.M. Lattimer, Phys. Rev. D 58 (1998) 013009.
[16] G.Y. Shao, Phys. Lett. B 704 (2011) 343.
[17] D.P. Menezes, M. Benghi Pinto, S.S. Avancini, C. Providência, Phys. Rev. C 79 (2009) 035807; 80 (2009) 065805.
[18] L. Woltjer, Astrophys. J. 140 (1964) 1309.
[19] T.A. Mihara, Nature (London) 346 (1990) 250.
[20] G. Chanmugam, Annu. Rev. Astron. Astrophys. 30 (1992) 143.
[21] D. Lai, S.L. Shapiro, Astrophys. J. 383 (1991) 745.
[22] E.J. Ferrer, V. de la Incera, J.P. Keith, I. Portillo, P.L. Springsteen, Phys. Rev. C 82 (2010) 065802;
E.J. Ferrer, V. de la Incera, Lect. Notes Phys. 871 (2013) 399.
[23] A.A. Isayev, J. Yang, Phys. Rev. C 84 (2011) 065802.
[24] A.A. Isayev, J. Yang, Phys. Lett. B 707 (2012) 163.
[25] A.A. Isayev, J. Yang, J. Phys. G 40 (2013) 035105.
[26] P.C. Chu, L.W. Chen, X. Wang, Phys. Rev. D 90 (2014) 063013.
[27] D. Bandyopadhyay, S. Chakrabarty, S. Pal, Phys. Rev. Lett. 79 (1997) 2176.
[28] D. Bandyopadhyay, S. Pal, S. Chakrabarty, J. Phys. G 24 (1998) 1647.
[29] P.C. Chu, L.W. Chen, Astrophys. J. 780 (2014) 135.
[30] P.C. Chu, X. Wang, L.W. Chen, M. Huang, Phys. Rev. D 91 (2015) 023003.
[31] G.N. Fowler, S. Raha, R.M. Weiner, Z. Phys. C 9 (1981) 271.
[32] S. Chakrabarty, S. Raha, B. Sinha, Phys. Lett. B 229 (1989) 112.
[33] S. Chakrabarty, Phys. Rev. D 43 (1991) 627; 48 (1993) 1409; 54 (1996) 1306.
[34] J.K. Teng, C.K. Wu, Chin. J. Electron. 25 (4) (2016) 726–733.
[35] O.G. Benvenuto, G. Lugones, Phys. Rev. D 51 (1995) 1989.
[36] G.X. Peng, H.C. Chiang, J.J. Yang, L. Li, B. Liu, Phys. Rev. C 61 (1999) 015201.
[37] G.X. Peng, H.C. Chiang, B.S. Zou, P.Z. Ning, S.J. Luo, Phys. Rev. C 62 (2000) 025801.
[38] G.X. Peng, A. Li, U. Lombardo, Phys. Rev. C 77 (2008) 065807.
[39] A. Li, G.X. Peng, J.F. Lu, Res. Astron. Astrophys. 11 (2011) 482.
[40] M. Di Toro, A. Drago, T. Gaitanos, V. Greco, A. Lavagno, Nucl. Phys. A 775 (2006) 102.
[41] G. Pagliara, J. Schaffner-Bielich, Phys. Rev. D 81 (2010) 094024.
[42] M. Di Toro, V. Baran, M. Colonna, V. Greco, J. Phys. G 37 (2010) 083101.
[43] G.Y. Shao, M. Colonna, M. Di Toro, B. Liu, F. Matera, Phys. Rev. D 85 (2012) 114017.
[44] X.J. Wen, X.H. Zhong, G.X. Peng, P.N. Shen, P.Z. Ning, Phys. Rev. C 72 (2005) 015204.
[45] Y. Zhang, R.K. Su, Phys. Rev. C 67 (2003) 015202.
[46] A. Ukawa, in: G. Kilcup, S. Sharpe (Eds.), Proceedings of the 1993 Uehling Summer School: Phenomenology and Lattice QCD, World Scientific, Singapore, 1993, p. 231.
[47] Zoltan Fodor, Sandor D. Katz, J. High Energy Phys. 03 (2002) 014.
[48] L.D. Landau, E.M. Lifshitz, Quantum Mechanics, 1965.
[49] A. Rabhi, H. Pais, P.K. Panda, C. Providência, J. Phys. G 36 (2009) 115204.
[50] X.J. Wen, S.Z. Su, D.H. Yang, G.X. Peng, Phys. Rev. D 86 (2012) 034006.
[51] X.J. Wen, Phys. Rev. D 88 (2013) 034031.
[52] R.C. Duncan, arXiv:astro-ph/0002442, 2000.
[53] C.Y. Ryu, K.S. Kim, M.K. Cheoun, Phys. Rev. C 82 (2010) 025804.
[54] C.Y. Ryu, M.K. Cheoun, T. Kajino, T. Maruyama, G.J. Mathews, Astropart. Phys. 38 (2012) 25.
[55] J.R. Oppenheimer, G.M. Volkoff, Phys. Rev. 33 (1939) 374.
[56] A.W. Steiner, M. Prakash, J.M. Lattimer, Phys. Lett. B 509 (2001) 10.
[57] J. Antoniadis, et al., Science 340 (2013) 6131.
[58] A.A. Isayev, Phys. Rev. C 91 (2015) 015208.
[59] P.C. Chu, L.W. Chen, Phys. Rev. D 96 (2017) 083019.
[60] B.A. Li, L.W. Chen, C.M. Ko, Phys. Rep. 464 (2008) 113.